Available online at www.sciencedirect.com
SCIENCE DIRECT®
Carbon 43 (2005) 994–1000
CARBON
www.elsevier.com/locate/carbon

Long-time low-impact ball milling of multi-wall carbon nanotubes

Ákos Kukovecz, Tímea Kanyó, Zoltán Kónya *, Imre Kiricsi

Department of Applied and Environmental Chemistry, University of Szeged, H-6720 Szeged, Rerrich Béla tér 1, Hungary

Received 5 July 2004; accepted 18 November 2004
Available online 6 January 2005

Abstract

A systematic study on the morphological changes experienced by multi-wall carbon nanotubes during long-time ball milling in a vibrating mill was performed. Samples were collected in the time interval 0 200 h and analyzed with TEM and N_2 adsorption. The change of the mean nanotube length with time could be approximated with a second-order exponential decay function. The length distribution function changed from the original log-normal to normal after 140 h of milling. Specific surface area, surface fractal dimension, the dimension of the capillary condensation and the pore size distribution (PSD) curve were calculated from the N_2 adsorption isotherms. These morphological descriptors all experienced characteristic changes after ~40 h of milling: the specific surface area decreased, the fractal dimension increased and the maximum of the PSD curve shifted downwards by ~0.5 nm. Results indicate that ball milling of carbon nanotubes is a rather complex process and that it can cause several morphological changes to samples besides the well-known cutting effect.
© 2004 Elsevier Ltd. All rights reserved.

Keywords: Carbon nanotubes; Grinding; Adsorption, electron microscopy; Fracture

1. Introduction

Multi-wall carbon nanotubes (MWCNTs) can be produced economically using the catalytic chemical vapor deposition (CCVD) method in quantities exceeding the capabilities of contemporary state-of-the-art single-wall carbon nanotube (SWCNT) synthesis techniques [1,2] by at least one order of magnitude. Therefore, many material-demanding applications of carbon nanotubes (e.g. polymer reinforcement) use MWCNTs [3] and information concerning the tailoring [4] of nanotube properties is highly sought after by the community [5,6].

Variants of the ball milling process have been previously applied to modify the length [7,8], particle size distribution [9], hydrogen adsorption properties [10] and lithium intercalation capacity [11] of carbon nanotubes as well as to perform carbon nanoparticle synthesis [12]. We have recently analyzed potential MWCNT ball milling cleavage mechanisms on the basis of HRTEM (High Resolution Transmission Electron Microscopy) tube end morphology observations [13]. Most of these studies utilized high impact mills and witnessed important changes in nanotube morphology within 24 h, even when the milling experiment itself was continued longer. In the present study we take a different approach and survey the possibilities of using a low impact vibrating mill for a longer time. In addition to TEM analysis we also carried out N_2 adsorption measurements and analyzed the obtained isotherms with respect to morphological descriptors like surface fractal dimension and the dimension of the capillary condensation. To our best knowledge this is the first report in the literature establishing a relationship between nanotube ball milling times and detailed N_2 adsorption characteristics.

* Corresponding author. Tel.: +36 62 544 620; fax: +36 62 544 619.
E-mail address: konya@chem.u-szeged.hu (Z. Kónya).

0008-6223/$ - see front matter © 2004 Elsevier Ltd. All rights reserved.
doi:10.1016/j.carbon.2004.11.030

Samsung Ex. 1039, Page 1 of 7
Samsung Electronics Co., Ltd., et al. v. Molecular Rebar Design, LLC
IPR2025-00356

2. Experimental

2.1. Carbon nanotube synthesis

Multi-wall carbon nanotubes were synthesized by CCVD utilizing a method reported previously [14]. Briefly, we used a Co-Fe/Al$(OH)_3$ (2.5–2.5 wt.% metal loading) catalyst prepared by the impregnation of aluminum-hydroxide (Aldrich) with aqueous metal-acetate solution. 5 g catalyst was spread as a 2 mm thin layer on a quartz boat and placed into a preheated horizontal tube furnace, then the system was purged with N_2 (120 ml/min) for 1 h and finally, the decomposition of acetylene (20 ml/min in N_2) was performed for 1 h at 973 K. After the reaction the catalyst support was removed in cc. NaOH, metal particles were dissolved in cc. HCl and the sample was purified of amorphous carbon in 0.1 M H_2SO_4 containing 0.1 M equivalent (relative to the amount of carbon) $KMnO_4$.

2.2. Ball milling

Two cylindrical stainless steel drums measuring 9.5 cm × 11 cm (height × diameter) and containing 110–110 small stainless steel balls were filled with 25 g MWCNT powder each. The diameter and mass distribution of the balls could be approximated as normal with parameters $m_{dia} = 0.707$ cm, $\sigma_{dia} = 0.005$ cm and $m_{mass} = 1.429$ g, $\sigma_{mass} = 0.027$ g, respectively. Prior to the milling procedure the drums were heated in flowing N_2 at 423 K for 1 h to remove water and adsorbed contaminants. The drums were placed into a vibrational mill horizontally and driven with an eccentric shaft at 50 Hz. Samples were taken from the two drums in an alternating pattern, 0.5 g at a time, at milling times 0.1, 0.2, 0.5, 1, 2, 5, 10, 20, 40, 60, 80, 100, 120, 140, 170 and 200 h.

2.3. Sample characterization

Transmission Electron Microscope (TEM) images were recorded on a Phillips CM10 instrument. Diluted suspensions of the samples in methanol were prepared and drop-dried on holey carbon coated copper TEM grids. Several TEM micrographs were recorded for each sample and analyzed for length and diameter distribution using the ImageJ image analysis software. 100 measurements were taken for each milling time. Nitrogen adsorption isotherms were measured at 77 K with a QuantaChrome Nova 2000 surface area analyzer. Samples were outgassed at 423 K for 1 h to remove adsorbed contaminants prior to the measurement. The correctness of using N_2 adsorption for the study of porous carbonaceous systems was validated by the theoretical work of Cascarini de Torre and Bottani [15]. The specific surface area (A^S_{BET}) was calculated using the multipoint BET method [16] on six points of the adsorption isotherm near monolayer coverage. Pore size distribution (PSD) curves were calculated from the adsorption branch of the isotherms using the Barrett–Joyner–Halenda (BJH) method [17]. The adsorption branch was favored over the desorption branch in order to avoid the tensile strength effect (TSE) artifact which very often complicates the PSD determination in mesoporous systems [18]. Surface fractal dimension (D_S) was calculated using the Frenkel–Halsey–Hill (FHH) method [19] from adsorption data near monolayer coverage [20]. Additionally, the Neimark–Kiselev method [21] was also utilized to calculate a fractal dimension value from the capillary condensation region of the adsorption isotherm (D_{CC}). For a more detailed theoretical treatment of the interpretation of N_2 adsorption isotherms we refer to the recent works of Ehrburger-Dolle [22] and Terzyk et al. [23]. It is enough to note here that the main difference between the conventional BET model of multilayer adsorption and the fractal FHH model is that the latter assumes that substrate–adsorbate interactions dominate over the adsorbate–adsorbate interactions, and are, therefore, non-negligible all the way out to the outermost layer of the film.

3. Results and discussion

The most evident macroscopic effect of ball milling was the fast increase of the apparent sample density. The originally fluffy and thin ($\rho_{apparent} = 0.07$ g/cm^3) starting material transformed into a dense black powder ($\rho_{apparent} = 0.38$ g/cm^3) after ~1 h of milling and kept this form until the end of the experiment. It is generally agreed [8] that this thickening is due to the loss of air trapped within the intertube space of the nanotube aggregates.

TEM images of the purified MWCNT material before milling as well as after 1, 40, 80, 140 and 200 h are presented in Fig. 1. It is evident that the nanotube length decreases with increasing milling time. Moreover, the entanglement of the tubes is also reduced as the nanotubes spend more time in the mill. This finding is in agreement with previous literature observations [8,10] and is explained by the reduction of the characteristic nanotube length. The amount of amorphous carbon and non-nanotube nanoparticles increased steadily with the grinding time. However, even after 200 h in the mill (Fig. 1F) the nanotube walls appear to be very similar to those observed in the beginning of the grinding. Even though previous high-impact milling studies [10] witnessed a different behavior, the nanotubes milled for 200 h in the present report appear to be clean-cut and well separated from the nanoparticles. We attribute this beneficial feature to the use of the low-impact mill.

Samsung Ex. 1039, Page 2 of 7
Samsung Electronics Co., Ltd., et al. v. Molecular Rebar Design, LLC
IPR2025-00356

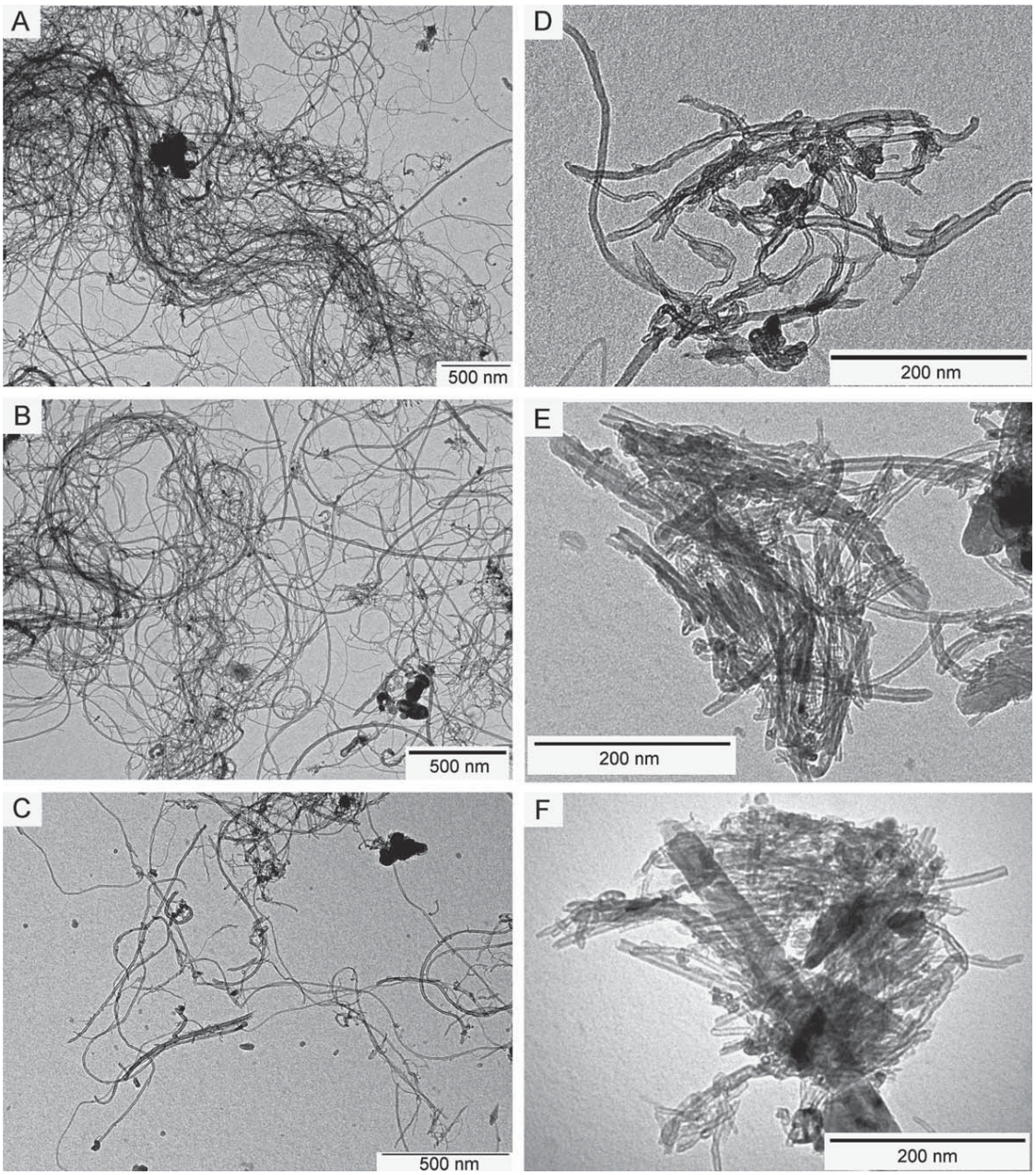

Fig. 1. Representative TEM micrographs showing the progress of the nanotube breaking process during long-time ball milling. Image A shows the starting material and pictures B–F correspond to milling times 1, 40, 80, 140 and 200 h, respectively.

Nanotube length distribution histograms corresponding to the TEM images of Fig. 1. are presented in Fig. 2. It should be noted that because of the large aspect ratio of the as-synthesized nanotubes and the limitations of the TEM instrument, exact length measurements on long MWCNTs (over 2 μm in our case) are rather difficult. Therefore, it is possible that our starting material contained tubes over 5 μm in length but these are not included in the histogram because of their unreliable length measurements. The length distribution of the starting material could be fitted well with the log-normal distribution. It is interesting to mention here that Geohegan et al. observed a similar length distribution in as-synthesized SWCNT samples prepared by the laser ablation method [24]. The length distribution became narrower with increasing milling times and could be fitted best with the log-normal distribution until ~80 h in the mill, after which the usage of the normal distribution appears to be more appropriate.

In Fig. 3. we present the mean nanotube length as a function of milling time. The length decreased from over 2 μm to approx. 950 nm in the first 2 h of the milling, then the rate of change became lower and quasi linear. We could achieve mean lengths of 500, 200 and

Samsung Ex. 1039, Page 3 of 7
Samsung Electronics Co., Ltd., et al. v. Molecular Rebar Design, LLC
IPR2025-00356

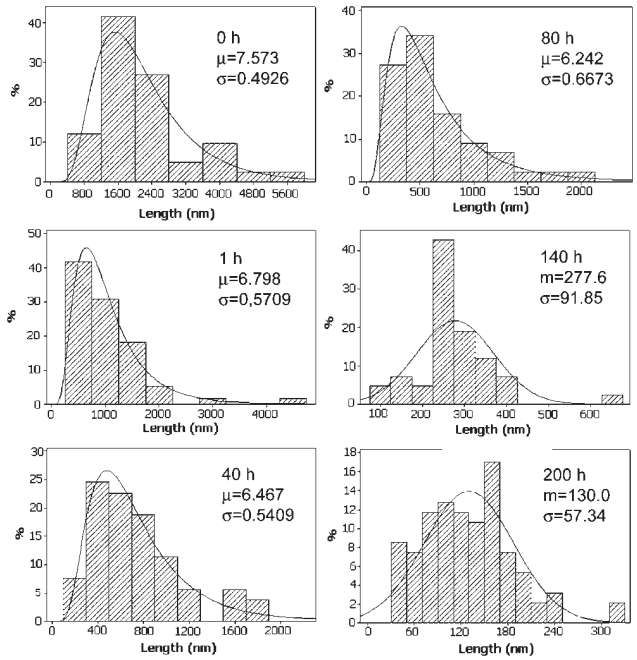

Fig. 2. Selected length distributions of ball milled SWCNT samples. The continuous line in each graph denotes the distribution function fitted to the experimental data. Histograms corresponding to milling times 0, 1, 40 and 80 h were fitted with log-normal distribution characterized by the scale parameter μ and the shape parameter σ, while length distributions obtained for 140 and 200 h milling were fitted by normal distribution characterized by the mean m and standard deviation σ.

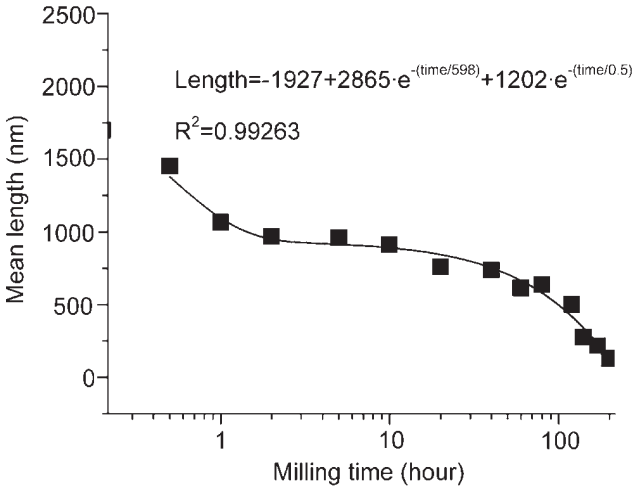

Fig. 3. Change of the mean nanotube length as a function of milling time. The continuous line shows a second-order exponential decay model fit of the experimental data, the fitting equation and the goodness-of-fit parameter are given in the figure.

140 nm after 120, 170 and 200 h of grinding, respectively. The whole MWCNT mean length vs. time in mill function could be fitted adequately with a second-order exponential decay function.

The next question is if the nanotubes experience any changes besides cutting during ball milling. In Fig. 4 three representative tube outer diameter distributions measured at 0, 100 and 200 h are compared. The distribution can be approximated as normal in each case. Albeit the fitted mean diameter increases slightly with milling time, pairwise two sample t-tests indicate that the three distributions can be considered equal at 95% confidence level. Therefore, we conclude that long-time ball milling does not alter the diameter distribution of MWCNTs.

Some basic morphological descriptors are readily obtained from N_2 adsorption isotherms. In Fig. 5 we depict the specific surface area (A^{S}_{BET}), the surface fractal dimension (D_S) and the dimension of the capillary condensation (D_{CC}) as the function of grinding time. A first glance at the magnitude of the data reveals that the samples (i) have large surface area (A^{S}_{BET}: 250–310 m^2/g), (ii) classify as surface fractals (D_S: 2.36–2.50) and (iii) are disordered to a large extent. The latter conclusion is derived from the small (<3.2) D_{CC} values following the interpretation of Pomonis et al. [25] who associated higher D_{CC} values with more ordered pore systems. These findings are in good agreement with literature reports as well as with our own previous MWCNT results [26]. It is very rewarding to analyze the small-scale changes of these three descriptors as functions of milling time. At the very beginning of the grinding process the specific surface area quickly increases by 10%, then remains constant for 10 h and finally drops more than 10% below the starting value. A possible interpretation of this behavior is as follows. The acidic oxidative purification leaves some of the nanotubes capped. When the mill is started, all tubes quickly break at least once, thus the inner pores of the originally closed MWCNTs become accessible for N_2. Further grinding reduces the length of the nanotubes without generating new surfaces, therefore, A^{S}_{BET} is retained. In the course of the milling the tube ends flatten and sometimes even close [13] resulting in a smaller specific surface area. Moreover, the tube entanglement is significantly reduced as the MWCNTs get shorter and consequently, less N_2 can be held in the intertube space. We assign the sharp drop in A^{S}_{BET} observed after ~100 h in the mill primarily to this latter effect.

Surface fractal dimension (D_S) monitors the self-similarity of the nanotube surface. In the case of multi-wall carbon nanotubes it can be interpreted as a measure of surface irregularities, local wells, carbon deposits etc. found at the outer surface of the tubes. On this basis we explain the increasing D_S values with the increasing roughness of the surface. It is worth pointing out an important difference between high impact ball milling and our long-duration low-impact procedure: while the former smashes MWCNT walls completely [10], the latter introduces gentler modifications to the surface which

Samsung Ex. 1039, Page 4 of 7
Samsung Electronics Co., Ltd., et al. v. Molecular Rebar Design, LLC
IPR2025-00356

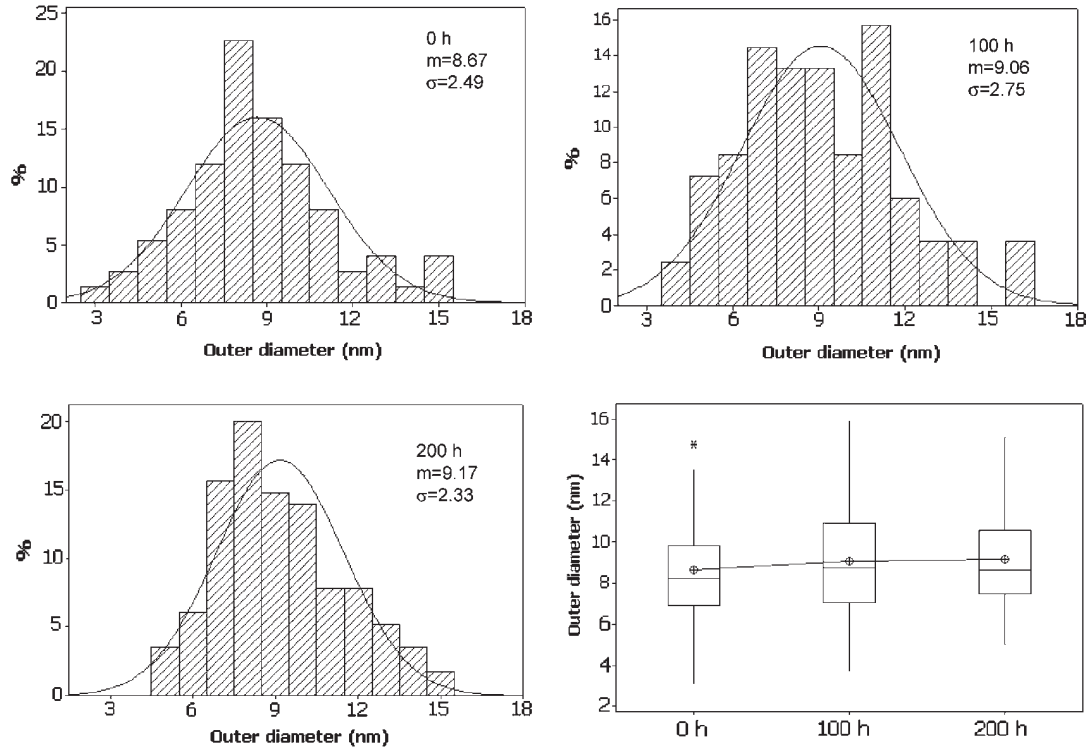

Fig. 4. Representative nanotube outer diameter distributions calculated for the starting material (0 h) as well as for 100 h and 200 h milling times. The diameter distribution can be approximated as normal in each case, the fitted mean diameter and standard deviation are given in the graphs. The interquartile box plot in the lower right corner allows the quick comparison of the distributions. Medians are marked with a horizontal line, sample means by encircled crosses and outlier values by an asterisk.

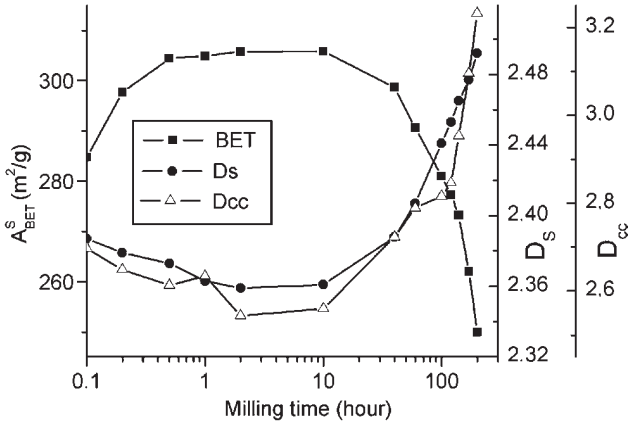

Fig. 5. Morphological parameters (specific surface area: left y axis, surface fractal dimension: right y axis, dimension of the capillary condensation: far right y axis) as a function of milling time, calculated from the N_2 adsorption isotherm.

are only detectable by surface fractal dimension analysis since they are not visible by TEM (Fig. 1F). This opens up surface fine-tuning possibilities that may prove beneficial in e.g. composite reinforcement nanotube applications.

Porous materials possessing a well-defined uniform channel system exhibit capillary condensation dimension (D_{CC}) values above 10 (e.g. Si-MCM-41) [27]. Smaller figures indicate less order in the material. Carbon nanotube samples with their relatively broad inner pore diameter distribution, partially closed ends and complex intertube openings generally classify as small D_{CC} materials. However, in Fig. 5 a noticeable 20% increase in D_{CC} is observed between 10 h and 200 h in the mill. On the basis of the TEM micrographs as well as the pronounced A^S_{BET} drop we suggest that the higher D_{CC} values originate from the MWCNT disentanglement: as the tubes get shorter, the structure of the nanotube sets is simplified and thus the overall pore structure appears slightly more ordered when probed with N_2 adsorption.

Pore size distribution (PSD) curves of the ground samples are presented in Fig. 6. As expected from TEM, the maximum of the PSD curves is at ~2.8 nm and in the beginning its position is independent of milling time. However, after 20 h in the mill the PSD curve starts broadening and its maximum shifts downwards: 2.5 nm at 100 h and 2.3 nm at 200 h. This is a somewhat intriguing finding since the outer diameter distribution was found to be unaffected by long-time ball milling (Fig. 4). A possible explanation can be offered on the basis of our previous HRTEM studies [13] which pointed out the importance of tube end morphology in general and that of the common MWCNT end flattening and partial

Samsung Ex. 1039, Page 5 of 7
Samsung Electronics Co., Ltd., et al. v. Molecular Rebar Design, LLC
IPR2025-00356

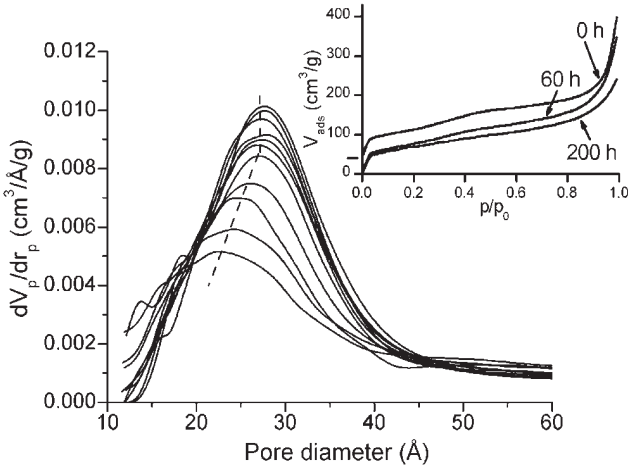

Fig. 6. Representative pore size distribution (PSD) curves of the milled MWCNT samples, calculated from the adsorption branch of the N_2 adsorption isotherm using the BJH method. PSD curves from top to bottom are derived from samples milled for 0.0, 0.1, 1, 5, 10, 20, 40, 60, 100, 140 and 200 h, respectively. The dashed line connecting the maxima of the PSD curves is a guide for the eye. The inset shows three representative N_2 adsorption isotherms measured after 0, 60 and 200 h of milling. The isotherm of the starting material ("0 h") is shifted upwards along the *y* axis by 40 units for clarity.

closure in particular. When the ball milling is started, the dominant event in the drum is the cutting of very long nanotubes into a few smaller segments. At this early stage there are relatively few nanotube ends in the sample and the probability of multiple ball impact on a chosen end is small. Therefore, the PSD curve is unaltered. As the nanotube shortening continues, the samples contain more and more tube ends and chances are that several of these have already been hit multiple times by a steel ball initiating end closure. The gross effect is that deformed pore endings start governing the adsorption properties which is evidenced both by the PSD maximum shift and the decrease of the specific surface area.

Let us emphasize here that the transition from the steep to the gentle nanotube length decrease rate (Fig. 3), the starting point of the A^{S}_{BET} decrease, the starting point of the pronounced increase of D_S and D_{CC} and that of the shifting of the PSD maxima coincide at ~10–20 h of milling time. We postulate that low-impact MWCNT ball milling experiments all go through such a critical point where several morphological descriptors start changing simultaneously. The exact time required for the transition probably depends on (i) the quality of the starting material, (ii) the geometry of the mill, (iii) the number and size distribution of the balls and (iv) on the frequency of the driving shaft.

4. Conclusion

We investigated the effects of long-duration low-impact ball milling on multi-wall carbon nanotubes with the aim of establishing relationships that can help in the application oriented tailoring of MWCNT properties. Ball milling cuts the nanotubes into shorter segments obeying a second-order exponential length decrease rule. The starting log-normal tube length distribution changes into normal after ~80 h. The outer diameter distribution is normal and is unaffected by the milling. Morphological descriptors calculated from N_2 adsorption isotherms change in a corresponding fashion at a critical point in time (~10 h in our experimental setup). We were able to offer a comprehensive explanation of the observed phenomena on the basis of nanotube disentanglement and tube end morphology changes. Even though it takes more time to reach a desired average nanotube length with low-impact ball milling than with conventional high-impact instruments, the former method is less destructive and allows a more precise tuning of nanotube properties.

Acknowledgments

Financial support of the Hungarian Ministry of Education through grants OTKA F046361, T046491 and F038249 is acknowledged. Á.K. and Z.K. thank the support of the Zoltán Magyary and the János Bólyai Postdoctoral Fellowships, respectively. ImageJ 1.31v is a public domain image analysis program for the Java platform developed by W. Rasband, National Institutes of Health, USA.

References

[1] Endo M, Hayashi T, Kim YA, Muramatu H, Ezaka M, Watts PCP, et al. A possible route to large-scale production of SWNTs through a combination of the substrate and floating catalyst methods. J Nanosci Nanotechnol 2004;4:132–5.
[2] Lyu SC, Liu BC, Lee SH, Park CY, Kang HK, Yang CW, et al. Large-scale synthesis of high-quality single-walled carbon nanotubes by catalytic decomposition of ethylene. J Phys Chem B 2004;108:1613–6.
[3] Velasco-Santos C, Martinez-Hernandez AL, Fisher FT, Ruoff R, Castano VM. Improvement of thermal and mechanical properties of carbon nanotube composites through chemical functionalization. Chem Mater 2003;15:4470–5.
[4] Kavan L, Dunsch L, Kataura H. Electrochemical tuning of electronic structure of carbon nanotubes and fullerene peapods. Carbon 2004;42:1011–9.
[5] Basiuk EV, Monroy-Pelaez M, Puente-Lee I, Basiuk VA. Direct solvent-free amination of closed-cap carbon nanotubes: a link to fullerene chemistry. Nano Lett 2004;4:863–6.
[6] Sveningsson M, Morian RE, Nerushev O, Campbell EEB. Electron field emission from multi-walled carbon nanotubes. Carbon 2004;42:1165–8.
[7] Pierard N, Fonseca A, Konya Z, Willems I, Van Tendeloo G, B.Nagy J. Production of short carbon nanotubes with open tips by ball milling. Chem Phys Lett 2001;335:1–8.
[8] Kim YA, Hayashi T, Fukai Y, Endo M, Yanagisawa T, Dresselhaus MS. Effect of ball milling on morphology of cup-stacked carbon nanotubes. Chem Phys Lett 2002;355:279–84.

Samsung Ex. 1039, Page 6 of 7
Samsung Electronics Co., Ltd., et al. v. Molecular Rebar Design, LLC
IPR2025-00356

[9] Wang Y, Wu J, Wei F. A treatment method to give separated multi-walled carbon nanotubes with high purity, high crystallization and a large aspect ratio. Carbon 2003;41:2939–48.
[10] Liu F, Zhang X, Cheng J, Tu J, Kong F, Huang W, et al. Preparation of short carbon nanotubes by mechanical ball milling and their hydrogen adsorption behavior. Carbon 2003;41: 2527–32.
[11] Gao B, Bower C, Lorentzen JD, Fleming L, Kleinhammes A, Tang XP, et al. Enhanced saturation lithium composition in ball-milled single-walled carbon nanotubes. Chem Phys Lett 2000;327:69–75.
[12] Li YB, Wei BQ, Liang J, Yu Q, Wu DH. Transformation of carbon nanotubes to nanoparticles by ball milling process. Carbon 1999;37:493–7.
[13] Kónya Z, Zhu J, Niesz K, Méhn D, Kiricsi I. End morphology of ball milled carbon nanotubes. Carbon 2004;42:2001–8.
[14] Kukovecz Á, Kónya Z, Nagaraju N, Willems I, Tamási A, Fonseca A, et al. Catalytic synthesis of carbon nanotubes over Co, Fe and Ni containing conventional and sol–gel silica-aluminas. Phys Chem Chem Phys 2000;2:3071–6.
[15] de Torre LEC, Bottani EJ. N_2 adsorption on porous carbonaceous materials. Langmuir 1997;13:3499–507.
[16] Brunauer S, Emmett PH, Teller E. Adsorption of gases in multimolecular layers. J Am Chem Soc 1938;60:309–19.
[17] Barrett EP, Joyner LG, Halenda PP. The determination of pore volume and area distributions in porous substances. I. Computations from nitrogen isotherms. J Am Chem Soc 1951;73:373–80.
[18] Groen JC, Peffer LAA, Pérez-Ramírez J. Pore size determination in modified micro- and mesoporous materials. Pitfalls and limitations in gas adsorption data analysis. Micropor Mesopor Mater 2003;60:1–17.
[19] Pfeifer P, Wu YJ, Cole MW, Krim J. Multilayer adsorption on a fractally rough surface. Phys Rev Lett 1989;62:1997–2000.
[20] Tang P, Chew NYK, Chan HK, Raper JA. Limitations of determination of surface fractal dimension using N_2 adsorption isotherms and modified Frenkel–Halsey–Hill theory. Langmuir 2003;19:2632–8.
[21] Neimark A. A new approach to the determination of the surface fractal dimension of porous solids. Physica A 1992;191:258–62.
[22] Ehrburger-Dolle F. A new way to analyze adsorption isotherms. Langmuir 1999;15:6004–15.
[23] Terzyk AP, Gauden PA, Kowalczyk P. Fractal geometry concept in physical adsorption on solids. Arab J Sci Eng 2003;28:133–67.
[24] Geohegan DB, Schittenhelm H, Fan X, Pennycook SJ, Puretzky AA, Guillorn MA, et al. Condensed phase growth of single-wall carbon nanotubes from laser annealed nanoparticulates. Appl Phys Lett 2001;78:3307–9.
[25] Armatas GS, Salmas CE, Louloudi M, Androutsopoulos GP, Pomonis PJ. Relationships among pore size, connectivity, dimensionality of capillary condensation, and pore structure tortuosity of functionalized mesoporous silica. Langmuir 2003;19:3128–36.
[26] Kanyó T, Kónya Z, Kukovecz A, Berger F, Dékány I, Kiricsi I. Quantitative characterization of hydrophilic-hydrophobic properties of MWNTs surfaces. Langmuir 2004;20:1656–61.
[27] Kukovecz A, Kanyó T, Kónya Z, Kiricsi I. Morphological characterization of mesoporous carbon-silicate nanocomposites. Micropor Mesopor Mater, accepted for publication. doi:10. 1016/j.micromeso.2004.11.025.

Samsung Ex. 1039, Page 7 of 7
Samsung Electronics Co., Ltd., et al. v. Molecular Rebar Design, LLC
IPR2025-00356